

Investigation into the delivery and efficacy of a unique *Avena Sativa* (Oat) Lipid Extract using Raman spectroscopic, immuno-diagnostic led analysis and skin evaluation.

**Running Header:** Oat Lipid Extract Analysis

**Authors:** C. Dewis, J. Daybell, C. Maunsell, Oat Cosmetics, Southampton, United Kingdom

**Corresponding Author:**

Cara Dewis, 2 Venture Road, Southampton Science Park, Chilworth, Southampton, Hampshire SO16 7NP, UK.

Email: cd@oat.co.uk

Phone:+44 (0) 2380 767 228

**Email addresses of all authors:**

cd@oat.co.uk jd@oat.co.uk cm@oat.co.uk

**Key Words:** oat lipids, confocal Raman spectroscopy, Lipbarvis® transmission electron microscopy, skin barrier, phytoceramides

**Abstract**

**OBJECTIVES:** Oat lipids are rich in phytoceramides which include the glucosylceramides. In this investigation, we analysed and investigated the delivery of a specific Oat Lipid Extract derived from *Avena sativa*, comprising ‘skin identical’ ratios of sterol, fatty acids and phytoceramides. This investigation is the first reported preliminary investigation of oat lipids utilising confocal Raman spectroscopy for the identification of oat ceramides from *Avena sativa* supported by Lipbarvis® transmission electron microscopy (TEM) and immunofluorescent analysis.

**METHODS:** Oil lipid class compositions were determined by single-dimension double-development high-performance thin-layer chromatography (HPTLC). Analysis of the oxidative stability of the Oat Lipid Extract was performed by RapidOxy. Raman spectra of lipids were obtained by confocal Raman spectroscopy Xplora. The potential of Oat Lipid Extract to increase the ceramide content of human epidermis was measured using

confocal Raman spectroscopy and immunostaining using an ex-vivo Perfex<sup>TM</sup> human abdominoplasty model. Effects of Oat Lipid Extract on skin barrier function gene expression were evaluated using RT-qPCR technology in reconstructed human epidermis (RHE). Transmission electron microscopy using the Lipbarvis® and immunostaining technique was conducted on human skin derived suction blister following treatment for 8 weeks with OAT LIPID EXTRACT. Immunostaining of hyaluronic acid, occludin, and ceramides were also performed.

**RESULTS:** HPTLC and GLC profiling of Oat Lipid Extract, revealed that of the ceramide classes identified, skin identical sphingosine and phytosphingosine bases were also present. A total polar lipid content of 40% (mg/100g lipid) of which 4% classed as ‘ceramides’ comprised ceramides/hydroxyceramides (1.36%), Gycosyl inositol phosphoryl ceramides (1.32%), and Glucosylceramides (1.32%). Raman profiling of Oat Lipid Extract was well correlated with stratum corneum and viable epidermis profiles. Oat Lipid Extract induced a significant increase in explant neutral lipid content 5 days post application. Polar lipid content was increased by 18% on Day 1 which further increased to 60% on Day 5 post application. Ceramide content of the skin was significantly increased as compared to the control and immunostaining, with image analysis revealed an increase in stratum corneum thickness. Oat Lipid Extract induced slight up-regulation of the gene expression of HAS3, and was more significant as compared to standard oat oil. Lipbarvis® TEM and immunostaining showed significant increase in the length of the intercellular lipid lamellae in the stratum corneum and the amount of detectable hyaluronic acid and ceramides in the epidermis.

**CONCLUSIONS:** Oat ceramides in the form of Oat Lipid Extract can be effectively delivered into the stratum corneum. This preliminary Raman and Electron microscopy Lipbarvis® study has given good insight into the possibility of Oat Lipid Extract mimicking the structure and function of the skin’s barrier. Further studies are required to provide evidence of the liquid crystalline changes that occur, and the molecular arrangement in the stratum corneum remains to be investigated.

## Introduction

The skin's barrier function within the stratum corneum (SC) comprises a complex array of lipids and proteins as a means of protecting the skin and to prevent moisture loss [1,2]. Important factors of the SC lipid behaviour are related to the molecular structures of the lipids, such as the hydrocarbon chain lengths of the ceramides and free fatty acids and the presence of non-saturated free fatty acids [3]. The SC consists of corneocytes embedded in a lipid matrix which forms the only continuous penetration pathway through the SC, and is therefore crucial for the functionality of the barrier [4]. Key lipid classes involved in this process are the ceramides [5,6]. The skins lipid barrier comprises, ceramides, cholesterol and free fatty acids (FFA's). For the formation of the epidermal barrier, FFAs are essential for numerous processes notably the formation of the ceramides of the lipid barrier and to contribute to the structure of the lipid matrix [4]. In addition, cholesterol is required in that it is of fundamental importance for the correct dense lipid organisation of the barrier, and thus for barrier function [7].

Studies have shown that application of a mixture of cholesterol, ceramides, and essential/nonessential free fatty acids (FFAs) in an equimolar ratio enables normal barrier recovery, whereas any 3:1:1:1 ratio of these four ingredients accelerates barrier recovery [8,9]. Xerotic or dry skin is a common occurrence, worsening with age and environmental exposure, and in those skin conditions with a prevalence for dryness [10]. In chronologically aged skin, with decreased epidermal lipid synthesis, and particularly a reduction in cholesterol synthesis, a ratio of 3x-cholesterol to the other lipids was shown to be beneficial also [11]. Omega-hydroxyceramides are required for corneocyte lipid envelope formation and normal epidermal permeability barrier function [12]. Furthermore, it has been shown that lipoxygenases mediate the effect of the essential fatty acid linoleate [13]. This occurs in O-linoleoyl- $\omega$ -hydroxyceramide, which, after hydrolysis of the linoleate moiety, is covalently attached to protein via the free  $\omega$ -hydroxyl of the ceramide, thus, forming the corneocyte lipid envelope, a scaffold between lipid and protein that helps seal the barrier [13].

Emollient products containing various natural oils are essential to any moisturising formulation and may vary depending on the formulators approach. They are now being increasingly recognised for their benefit for a variety of skin diseases and the restoration of cutaneous equilibrium. Unique characteristics of various oils are important when considering their use for topical skin care [14]. Differing ratios of essential fatty acids are

major factors of the barrier repair effects of natural oils. Oils with a higher ratio of linoleic acid to oleic acid have stronger barrier repair potential, whereas oils with higher amounts of oleic acid may be detrimental to skin-barrier function, potentially resulting in skin irritation [15,16]. Isolating skin-identical ceramides with the correct stereochemical structures has long been a key desire for the development of effective skin care products.

Restoration of ceramides in depleted skin by phytoceramides from wheat and rice have been shown to provide a benefit in restoring an improvement in the skin's barrier [17,18]. Oats, and their varieties, are globally produced forming an important part of the diet for many people. [19,20]. Oats also possess a variety of beneficial activities especially its anti-inflammatory activity notable in many skin care products in the management of atopic dermatitis. Only in recent years has attention been given to the lipid content of oats, especially its phytoceramide content. Recent studies utilising HPTLC, have shown that glucosylceramides isolated from Ethiopian oat grain (*Avena abyssinica*) consist of C18-dihydroxy sphingoid bases amide-linked with  $\alpha$ - hydroxylated saturated fatty acids (C16-C24) and suggests them to be a potential source of ceramides (CER's) for skin benefits [21]. Furthermore, it has also been reported that oat lipid extract can activate PPARs and subsequently increase epidermal lipid synthesis and differentiation markers [22]. Oat lipid extracts have been shown to exhibit dual agonism for PPAR $\alpha$  and PPAR $\beta/\delta$  and increase direct PPAR target gene induction in primary human keratinocytes. Also, oat oil significantly increases ceramide levels (70%) suggesting a functional translation of PPAR activation by oat oil in keratinocytes and an improved skin barrier function [23].

For proper barrier functioning it is the stereochemical nature, sphingoid base structure, and fatty acid class which are inherent in the skin. Plants contain many so-called phytoceramides but their structure has never been described as skin-identical because of the varied differences in sphingoid bases, which give the rigidity and fluidity between the crystalline states. Furthermore, since cholesterol is not the predominant sterol in plants, unlike the skin, it is argued in the literature that the stereochemical structure of these phytoceramides may not be a replacement for a skin barrier depleted of 'true' ceramides. As such skin-identical lipid mixes are commercially available for skincare use, though these are considered expensive for wider applications, and are derived from bio-fermentation processing.

Several studies have described the isolation and identification of oat lipids and individual oat 'ceramides'. However, as described herein, this is the first reported preliminary

investigation of oat lipids utilising confocal Raman spectroscopy for the identification of oat ceramides from *Avena sativa*. In this investigation, we analysed a specific oat lipid extract, naturally extracted from *Avena sativa*, using ethanol, comprising ‘skin identical’ ratios of sterol, fatty acids and phytoceramides. Confocal Raman spectroscopy is a widely accepted sensitive approach for the study of the skin’s barrier in a space-resolved manner [23,26]. In order to gain a further understanding of the lipid nature and its effects on skin barrier lipids, we utilised a multi-method approach led by Raman spectroscopy, transmission electron microscopy (Lipbarvis®), and immunostaining, to ascertain the structure, and beneficial efficacy of Oat Lipid Extract, comprising a complex of ceramides, polyunsaturated fatty acids, sterols, phospholipids, triacylglycerols, tocopherols, tocotrienols and other polar lipids.

## Materials & Methods

Oat Lipid Extract is naturally derived from a previously unconsidered by-product of the fractionation of oat oil from the oat kernel. The by product is produced as a viscous residue during the extraction of oil from oats by fractionation with a polar solvent. Neutral and polar lipids may be separated from oats by extracting using a polar solvent such as ethanol, however high levels of residual solvents and sugars and low proportion of desirable skincare components make this an unusable ingredient in personal care. Oat Lipid Extract has been developed as an oat oil fraction which has been further refined, to contain high polar lipid content and other desirable components, but which does not contain significant water / solvent residue.

### Lipid profiling

Profiles of lipid classes and total amounts of Oat Lipid Extract were carried out using GLC and HPTLC.

*Lipid extraction and fatty acid analysis* - Oils were made up to 10mg.ml with Chloroform:Methanol and fatty acid methyl esters (FAME) were prepared by acid-catalysed trans-esterification of total lipids [27]. FAME were separated by gas-liquid chromatography using a ThermoFisher Trace GC 2000 (ThermoFisher, UK) equipped with a fused silica capillary column (ZBWax, 60m x 0.32 x 0.25 mm i.d.; Phenomenex, UK) with hydrogen as carrier gas and using on-column injection. The temperature gradient was

from 50 to 150°C at 40°C/min and then to 195°C at 1.5°C/min and finally to 220°C at 2°C/min. Individual methyl esters were identified by comparison to known standards (Supelco 37-FAME mix; Sigma-Aldrich Ltd., UK) and by reference to published data [28]. Data were collected and processed and fatty acid content per g of tissue was calculated using heptadecanoic acid (17:0) as an internal standard.

*Lipid class analyses* - Oil lipid class compositions were determined by single- dimension double-development high-performance thin-layer chromatography (HPTLC) using methyl acetate/propan-2-ol/chloroform/methanol/0.25% aqueous KC1 (25:25:25:10:9, by vol.) and hexane/diethyl ether/acetic acid (85:15; 1.5, by vol.) as first and second development solvents, respectively. Lipid classes were quantified by charring followed by calibrated scanning densitometry using a Camag 3 Scanner (Camag, Switzerland). Identities of individual classes were confirmed by comparison with reference to R<sub>f</sub> values of authentic standards.

### **Oxidative stability of OAT LIPID EXTRACT**

Analysis of the oxidative stability of the Oat Lipid Extract [29] was performed using the RapidOxy method (Anton Paar, Germany). Briefly, each test was performed under high oxygen pressure (7 bar initial pressure) at an elevated temperature of 140 °C. Sample oxidation was indicated by a fall in pressure inside the oxidation chamber to a selected level (20% of maximum pressure). The oxidation curve subsequently produced, is characterised by an Induction Period (IP), i.e., the time taken to reach the set decrease in pressure, and expressed in minutes. Results are the mean of duplicate tests performed on each sample.

### **Confocal Raman Spectroscopic lipid analysis**

Raman spectra were obtained using a confocal Raman spectroscopy Xplora (Horiba, Jobin Yvon) performed on 10 µm thick frozen skin sections in the presence of the test product using a 532 nm laser. A long focal microscope objective PL Fluotar L 100\_ /NA 0.75 WD 4.7 was used to focus the laser light on the surface of the sample and to collect the back scattered light. The collected light was filtered through a notch filter and dispersed with a 10 cm<sup>-1</sup> spectral resolution using a 100 mm slit and a holographic grating of 1200 grooves per mm. The confocal pinhole was set to 300 µm. The acquisition time was set to 10 s coupled with 5 accumulations for each analyzed points. The Raman Stokes signal was recorded with a Charge-Coupled Device detector (CCD camera).

Spectral acquisition was performed using LabSpec 6 software (Horiba Scientific). Raman measurements were performed on 4 to 6 points of the stratum corneum, the living epidermis and the tested product in the 400–3800 cm<sup>-1</sup> spectral range. For the analysis, CaF2 histological slides were used. All spectra were smoothed using LabSpec 6 software and the baseline was corrected using an automatic polynomial function and normalized using the whole spectrum. For each batch 2 frozen sections were analyzed and Raman measurements were performed on 5 different zones of the stratum corneum in the 400–3800 cm<sup>-1</sup> spectral range. On each zone 10 to 12 points have been analyzed and successively averaged. For the analysis, CaF2 histological slides were used. All spectra were smoothed using LabSpec 6 software and the baseline was corrected using an automatic polynomial function and normalized using the whole spectrum. Trans/Gauche conformers ratio was observed by calculating the I1060+I1130/I1080 ratio and the I2882/I2852. High values of these ratio are associated with a compact state in the lipid packing while a decrease is indicative of loosening [30].

*Skin Samples:* The potential of the Oat Lipid Extract to increase the ceramide content of human epidermis was measured using confocal Raman spectroscopy and immunostaining of human skin using an ex-vivo Perfex<sup>TM</sup> abdominoplasty model [31]. In addition, the effect on polar and neutral lipid content was also assessed. Skin explants (female Caucasian, 59 years old; 2 x 3.8 mm diameter) were held on a specifically designed support composed of a reservoir of culture medium surmounted by a grid on which the skin is stretched. The skin support was connected by a fluid circuit to a second reservoir of culture medium stored in the incubator at 37°C (high RH% + 5% CO<sub>2</sub>). Circulation of the culture medium was ensured by a peristaltic pump. On day 0 (D0), the test product was applied topically (9 µl/ explants (2mg/cm<sup>2</sup>)). Control explants received no treatment.

*Immunostaining:* After fixation for 24 hours in buffered formalin, skin samples were dehydrated and impregnated in paraffin using a Leica PEARL dehydration automat and then embedded using a Leica EG 1160 embedding station. 120 serial sections of 5 µm thickness were made using a Leica RM 2125 Minot-type microtome for each paraffinised sample, and sections were mounted on silanised histological glass slides Superfrost® UltraPlus. Microscopic observations were performed using a Leica DMLB or Olympus BX43 microscope, and images digitised using a numeric DP72 Olympus camera with CellID storing software.

Cell viability of epidermal and dermal structures were assessed by microscopic observations of paraffinised sections following Masson's trichrome staining, Goldner's variant [32]. Neutral lipids were stained on frozen skin sections (LipidTox® green neutral lipid, Life technologies). Sections were then fixed using a Ciaccio solution, post-chromatized and incubated with LipidToxTM, diluted at 1 :3000 in phosphate buffered saline (PBS), for 45 minutes at room temperature. Nuclei were counterstained with DAPI (Sigma) diluted at a concentration of 0,1 µg/mL in PBS. Staining was assessed by image analysis.

Polar lipids were stained on frozen sections using ReZolve-L1<sup>TM</sup> reagent (Rezolve scientific). Nuclei were counterstained with DAPI (Sigma) diluted at a concentration of 0,1 µg/mL in PBS. Staining was assessed by image analysis. Polar lipids were stained on frozen sections using Nile Red reagent diluted at a concentration of 0,1 µg/mL in PBS (Nile Red), in dark and at room temperature for 30 minutes. Ceramide immunostaining was performed on paraffin sections with anti-ceramide monoclonal antibody (Glycobiotech, clone S58-9) diluted at 1:25 in PBS, Bovine serum albumin (0.3%) and Tween 20 (0.05%) for 1 hour at room temperature, together with a biotin/ streptavidin amplifying system and revealed with VIP, a violet substrate of peroxidase (Vector).

### **Barrier Function - Gene Expression**

The effects of the Oat Lipid Extract compounds were evaluated using RT-qPCR technology in reconstructed human epidermis (RHE). Extracted mRNA was analyzed using a PCR array ("mQPA-NHEK-Barrier function and Hydration-32") for the analysis of 32 target genes (including 2 housekeeping genes) for their importance in keratinocyte physiology and hydration. Prior to this assay, a preliminary cytotoxicity assay was performed on normal human epidermal keratinocytes (NHEK) using a standard MTT reduction assay. Seven-day-old reconstructed human epidermis were topically treated with the test product (50 µl/RHE) and RHE were incubated for 3 days. Retinoic acid was used as a control. All experimental conditions were performed in duplicate. At the end of incubation, the RHE were washed in phosphate buffered saline solution (PBS) and immediately frozen at -80°C.

Samples were mechanically homogenised using a pestle and total RNA was extracted from each sample using TriPure Isolation ReagentR. The amount and quality of RNA was evaluated using electrophoresis (Bioanalyzer 2100, Agilent technologies). Complementary

DNA (cDNA) was synthesised by reverse transcription of total RNA in presence of oligo(dT) and Transcriptor Reverse Transcriptase (Roche). The cDNA quantities were then adjusted prior to PCR.

### **Lipid Lamellar Formation - Electron Microscopy Analysis (Lipbarvis®TEM)**

The effects of Oat Lipid Extract were further evaluated via Lipbarvis®transmission electron microscopy (Dähnhardt GmbH). Determination of length of lipid lamellae (electron microscopy analyses), immuno-histochemical analysis of hyaluronic acid, ceramides and occludin (light microscopy analysis) were also performed.

Oat Lipid Extract *Treatment and Suction Blisters*: According to Good Clinical Practice (GCP) the test product Oat Lipid Extract was applied to the forearms of six healthy female caucasian consenting volunteers willing to comply with the inclusion and exclusion criteria of the protocol. At the baseline visit to the study centre, one arm was treated and the other arm was left untreated in a randomised schema. The product was applied daily for 8 weeks with compliance checks every 2 weeks for application correctness and a diary. At the end of treatment, 7 mm suction blisters ( 3 per arm) were raised and removed. Samples were then frozen at minus 80°C.

*Transmission Electron Microscopy (Lipbarvis®TEM)*: One small part of each suction blister samples ( $\varnothing$  3 mm) was fixed overnight in Karnovsky's medium at 4°C, washed twice with 0.2M sodium cacodylate buffer for 10min each, and postfixed with 1% RuO<sub>4</sub> in 0,13M sodium cacodylate buffer at 4°C for 90 minutes. Specimens were then washed twice with aqua bidest, dehydrated in an ethanol series and embedded in epoxy resin. Polymerisation was carried out overnight at 60°C. Briefly, perpendicular sections of the suction blister samples were prepared with an ultramicrotome (Ultracut S Leica Microsystems, Wetzlar, Germany) using a diamond knife (35°, Diatomee, Switzerland). Sections were mounted onto copper grids. The subsequent counterstaining was carried out with uranyl acetate and lead citrate. For TEM examination a TEM CM 10 (FEI, Eindhoven, Netherlands) with an acceleration voltage of 80 kV was used. Images were captured with a CCD camera (IDS, Obersulm, Germany) connected directly to the TEM. In previous investigations we had found that — as long as the sample was chosen from within a homogeneous corneocyte layer — the samples provided a reproducible image of the stratum corneum structure.

In the images of the perpendicular sectioned stratum corneum a minimum of 5 areas between the corneocytes in different depth were chosen according to the following criteria: In healthy skin as well as in dry skin, an intercellular space (ICS) had to be framed by two corneocytes. Within the chosen areas an ICS ( $\text{nm}^2$ ) and inter-cellular lipid lamellae length (ICLL) (nm) were semi-automatically selected and marked using a software plug-in developed for the Image J software ([www.nih.gov](http://www.nih.gov)). In order to compare ICLL in the different samples the ratio ICLL/ICS was normalized to an area of 1.000 nm<sup>2</sup>. The normalized ICLLs (nICLL) were used for subsequent statistical analysis.

*Immuno-histochemical Analysis:* Suction blister samples were fixed in modified Karnovsky's fixative at 4°C to preserve antigenicity. Samples (3mm diameter punch biopsies, halved) were dehydrated in ethanol and embedded in LR-White, using a low temperature polymerisation. 200 nm sections were then prepared with an ultramicrotome (Ultracut S Leica Microsystems, Wetzlar, Germany) using a diamond knife (35°, Diatomee, Switzerland) and placed on round glass coverslips.

Sections were treated with 1% bovine serum albumin in washing buffer [0.1% Tween 20 in phosphate buffered saline] for 60 min in order to prevent nonspecific binding. The primary antibodies -anti-Hyaluronic Acid (Cloud Clone Corp.) and anti-Occludin (abcam), both diluted 1:15 in washing buffer, and -anti Ceramides antibody (EnzoLife Sciences) used undiluted, were applied onto the sections in a humid chamber at 4°C overnight. After washing four times with washing buffer the sections were incubated either with a Cy3-conjugated anti-rabbit or with an Alexa Fluor 488 conjugated anti-rabbit IgG secondary antibody (Dianova) (all diluted 1:500) for 180 minutes in darkness. The samples were washed again (five times), stained and embedded for visualisation of the nuclei with Roti®-Mount Fluor Care DAPI (Roth). Control samples were carried out without primary antibody application. Samples were analysed with a Leica fluorescence microscope (Leica DMLS). Images were taken with a coupled CCD Camera (ISH500 Tucsen) using the software ISIListen, Tucsen Photonics. Measurement of the fluorescence intensities was carried out using ImageJ software.

*Statistics:* Analysis of the study objectives was performed using Microsoft Excel and Statistica (StatSoft). Microsoft Excel was used for the calculation of the descriptive statistics, i.e., for calculating the relative data, mean values and standard deviations. In addition, Microsoft Excel was used for graphical visualisation of the collected data sets in bar charts presenting mean values alongside with error indicators corresponding to

standard deviations. The inductive analysis of the study objectives by hypothesis testing was carried out using Statistica. The Kolmogorov-Smirnov test was applied in order to check for normal distribution of the continuous data. Under the given requirement of normally distributed data series, the t-test for dependent samples was applied for analysing the significance of differences. The hypothesis of a normal distribution was accepted when there was a p-value > 0.05. Concerning the differences between the treatment situations, the significance level was set to a  $\alpha = 5\%$  cutoff. Consequently, in cases of a p-value  $\leq 0.05$ , the difference between the data series under comparison was accepted as statistically significant.

## Results

### Lipid Profiles

Fatty Acid Profile (from Neutral and Polar Fraction)	mg/100g
Myristic 14:0	0.07
Pentadecylic 15:0	0.08
Palmitic 16:0	4.66
Stearic 18:0	0.55
Arachidic 20:0	0.04
Behenic 22:0	0.04
<b>Total Saturated</b>	<b>5.45</b>
Palmitoleate 16:1n-9	0.02
Palmitoleic 16:1n-7	0.06
Oleic 18:1n-9	12.43
Vaccenic 18:1n-7	0.23
Eicosenoic 20:1n-9	0.24
<b>Total Monounsaturated</b>	<b>12.97</b>
Linoleic 18:2n-6	10.85
Eicosadienoic acid 20:2n-6	0.02
<b>Total n-6 PUFA</b>	<b>10.87</b>
Alpha-Linolenic 18:3n-3	0.35
Stearidonic acid 18:4n-3	0.03
<b>Total n-3 PUFA</b>	<b>0.38</b>
<b>Total Fatty Acids</b>	<b>29.67</b>
<b>Phospholipids</b>	
Phosphatidylcholine (PC)	6.0
Phosphatidylinositol (PI)	3.5
Phosphatidylethanolamine (PE)	3.0
Phosphatidic acid/Phosphatidylglycerol/cardiolipin (PG)	1.5
Lysophosphatidylcholine	1.0
<b>Total Phospholipids</b>	<b>15.00</b>
<b>Sterols</b>	
$\beta$ -sitosterol	4.0
Avenasterol	4.0
Other (including cholesterol)	2.0
<b>Total Sterols</b>	<b>10.0</b>
<b>Neutral Lipids</b>	
Triacylglycerols	37.0
Free fatty acids	11.0
Cholesterol/sterols	10.0
Diacylglycerol	2.0
<b>Total Neutral Lipids</b>	<b>60.0</b>

Table I: Total lipid and fatty acid content of Oat Lipid Extract

HPTLC and GLC indicate a total polar lipid content of 40mg/100g lipid of which 4% are classed as ‘ceramides’ comprising ceramides/hydroxyceramides (1.36%), Gycosyl inositol phosphoryl ceramides (1.32%), and Glucosylceramides (1.32%). Skin ceramides are divided into at least 12 classes of which there are hundreds of sub-species [33], and these account for 40-50% of the lipids in the stratum corneum. Further profiling of the Oat Lipid Extract, revealed that of the ceramide classes identified, skin identical sphingosine and phytosphingosine bases were also present (Table II).

Approximate Composition*	Percentage
Ceramides	1.36
Hydroxyceramides	
Glycosyl Inositol Phosphoryl Ceramides (Proceramide)	1.32
Glucosylceramide	1.32
<b>Total Ceramides</b>	<b>4.00</b>



Ceramide Class*	Oat Lipid Extract Skin Identical (%)	Oat Lipid Extract Total incl. Isomers (%)
Non-hydroxy-sphingosine [NS]	0.07	0.52
Non-hydroxy-phytosphingosine [NP]	0.13	0.13
Omegahydroxy-6-hydroxy-sphingosine [EOH]	0.47	0.47
Alphahydroxy-sphingosine [AS]	0.05	0.19
Alphahydroxy-phytosphingosine [AP]	0.05	0.05
<b>Total</b>	<b>0.78</b>	<b>1.36</b>

Table II: Ceramide classes present in Oat Lipid Extract

In addition a large proportion of phospholipids were also present (15mg/100g) with phosphatidylcholine being the most predominant species. The largest proportion of lipids present were identified as neutral lipids (60mg/100g) comprising triacylglycerols (37mg/100g), free fatty acids (11mg/100g), sterols (10mg/100g) and diacylglycerol (2mg/100g). Not surprisingly the sterols were identified mainly as  $\beta$ -sitosterol and avenasterol. Fatty acid profiling from neutral and polar fractions revealed relatively high amounts of both mono- and polyunsaturated fatty acids (12.97mg/100g and 10.87mg/100g respectively), as compared to saturated fatty acid content (5.45mg/100g).

### Oxidative Stability

The purpose was to identify the oxidative stability of the Oat Lipid Extract when compared with the standard oat and sunflower oils as controls [29]. The Oat Lipid Extract was observed to be far more stable than either the sunflower or oat oils with nearly a 3-fold increase in stability as compared to sunflower oil (Fig 1).

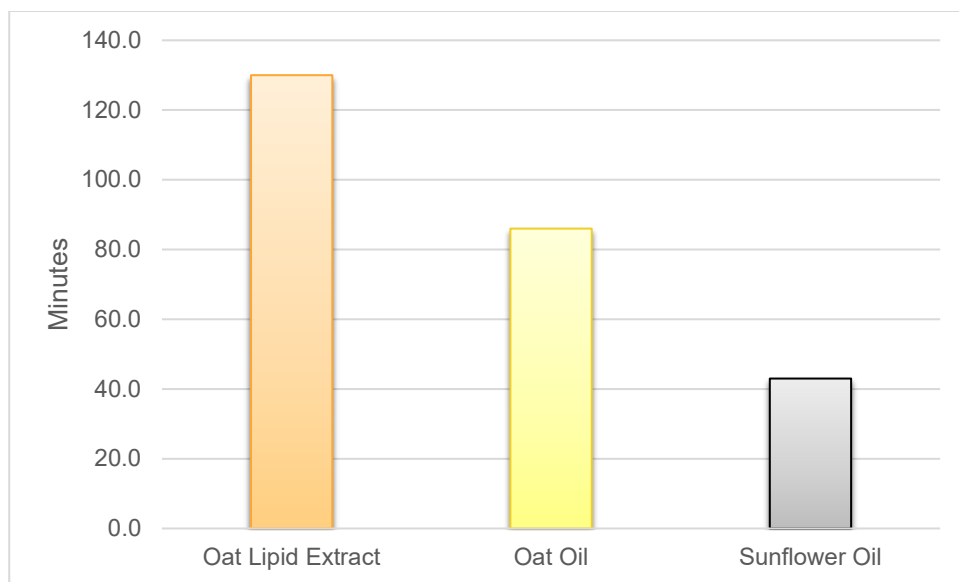


Figure 1: Marked oxidative stability of the Oat Lipid Extract measured by RapidOxy as compared to oat and sunflower seed oil respectively.

### Comparative Epidermal Lipid Content - Raman Spectroscopy

*Single application of Oat Lipid Extract to viable skin:* The Raman profile of the Oat Lipid Extract is shown in Fig 2. Comparisons are also shown to the Raman profiles of stratum corneum and viable epidermis. Under normal conditions, the lipids are organized in a

hexagonal phase. While maintaining a hexagonal organization characteristic of normal skin, the product significantly modifies the Trans/Gauche ratio.

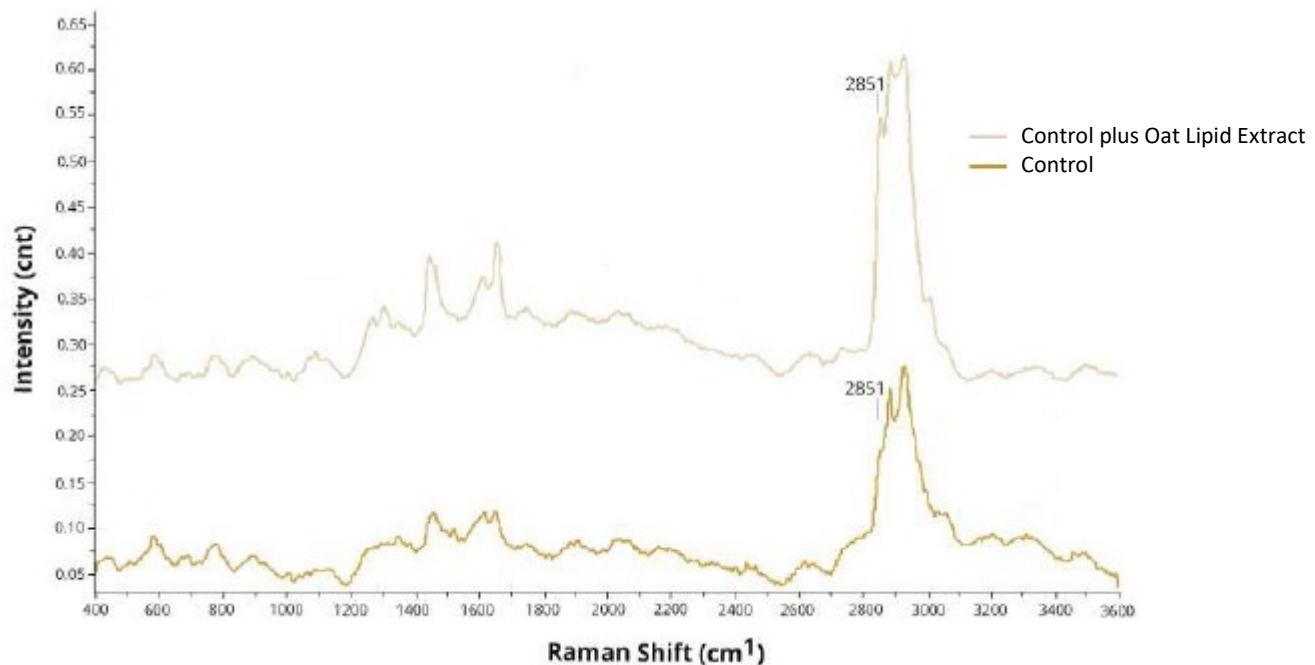


Figure 2: Confocal Raman spectrograph of a single application of oat lipid EXTRACT (top) to viable skin explants versus untreated control (bottom). Essential ceramides are identified at 2851 cm<sup>-1</sup>.

*Correlation of Oat Lipid Extract profile to skin:* A previous study (unpublished data) has shown that the Oat Lipid Extract contains lipids which are characterized by Raman peaks  $1060$  and  $1080\text{ cm}^{-1}$  but that there is no corresponding peak at  $1130\text{ cm}^{-1}$ . The product increases the amount of  $1060$  and  $1080$  lipids and then modifies the Trans/Gauche ratio so as to increase the fluidity of the stratum corneum lipids. Consequently, the Raman profile of the Oat Lipid Extract is well correlated with that of the stratum corneum and viable epidermis (Fig 3). Of particular importance are those peaks around  $500\text{ cm}^{-1}$  which relate to sterols; peaks around  $1003$  and  $1155$  which relate to phenolic antioxidants; and peaks around  $2851$  and  $2897$  which relate to ceramides. These peaks indicate that the Oat Lipid Extract is a good source of skin supplementing lipids.

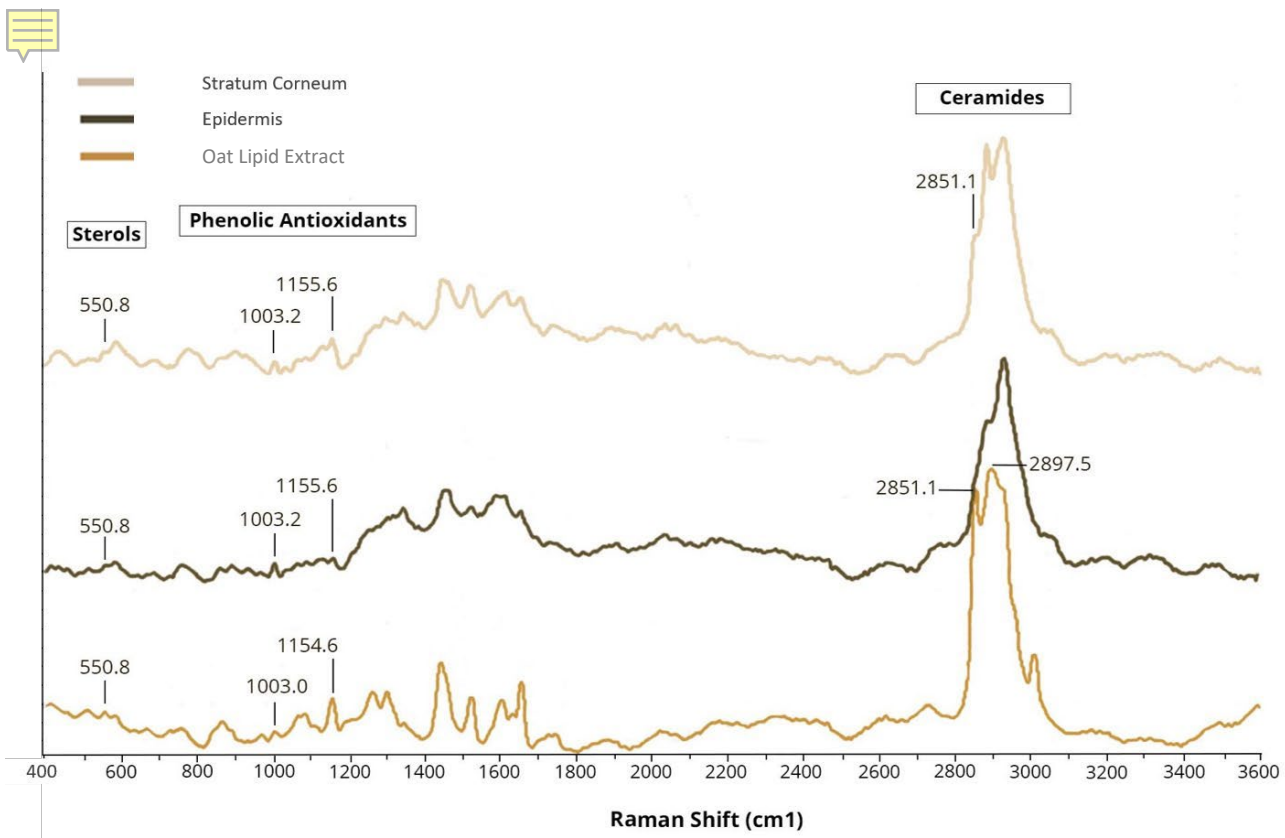
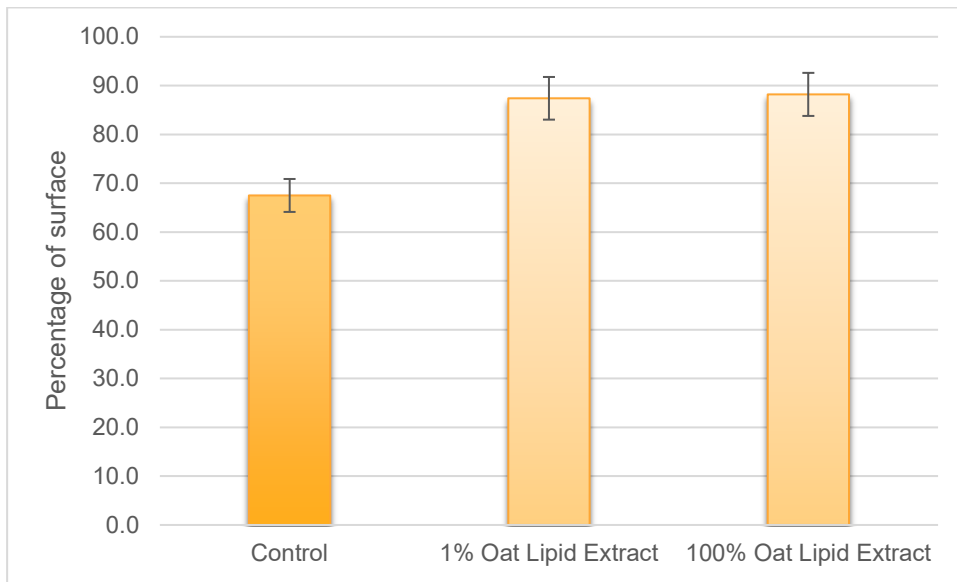


Figure 3: Confocal Raman spectrograph of a single application of Oat Lipid Extract to viable skin explants versus untreated control. Essential ceramides are identified at 2851 cm<sup>-1</sup>

### Comparative Epidermal Lipid Content - Immunostaining

Evaluation of the Oat Lipid Extract on the skin barrier and hydration in human explants by both Raman spectroscopy and immunostaining with image analysis, was carried out. No negative effects of the test product on cell viability was observed (data not shown).

Applications of 100% and 1% Oat Lipid Extract induce an increase in the neutral lipid content of the explants at day 5. More specifically, the application of 100% Oat Lipid Extract induces a 31% greater increase in neutral lipid content than the control, while that of 1% Oat Lipid Extract induces a 29% increase when drawing the same comparison. The differences between 100% and 1% Oat Lipid Extract is only very slight (Fig 4). Regarding polar lipid content, application of 100% Oat Lipid Extract induces an 18% increase in polar lipid content as compared to the control on Day 1. However, on day 5 this is increased to 60% when compared to the control sample (Fig 5). In a similar fashion (Fig 6), the ceramide content of the skin was increased as compared to the control. Furthermore, immunostaining and image analysis revealed an increase in stratum corneum thickness, with the Oat Lipid Extract ceramides replenishing those which had been depleted.



#### Measurement of the Neutral Lipid Surface at Day 5 (Shown in Green)

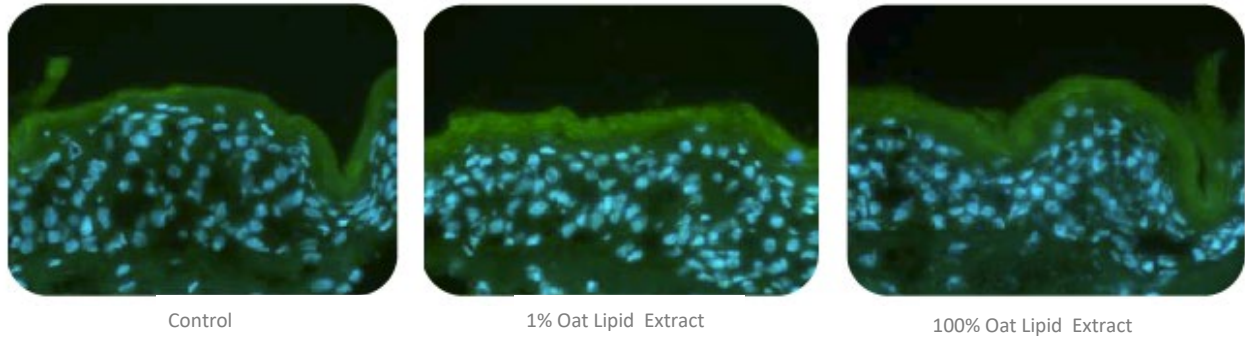
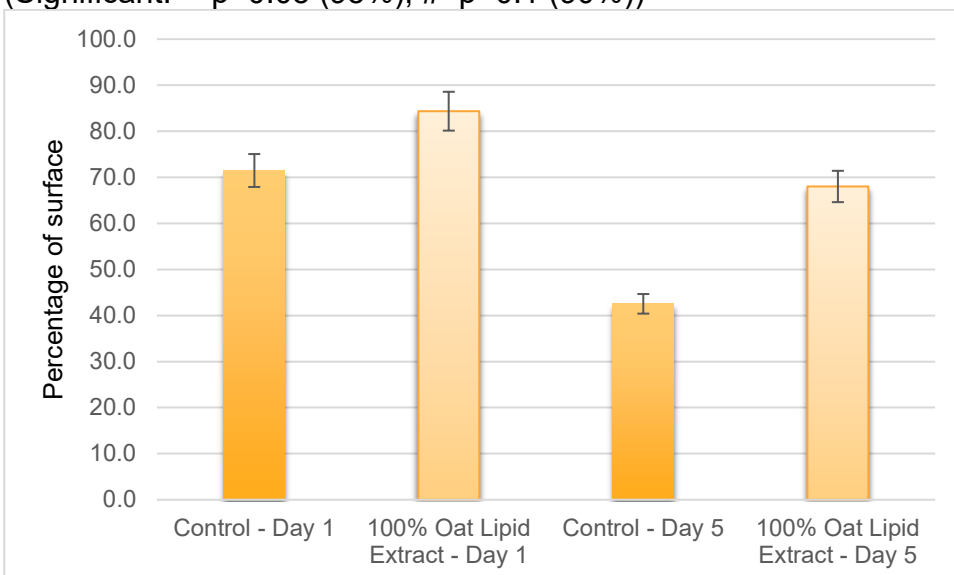
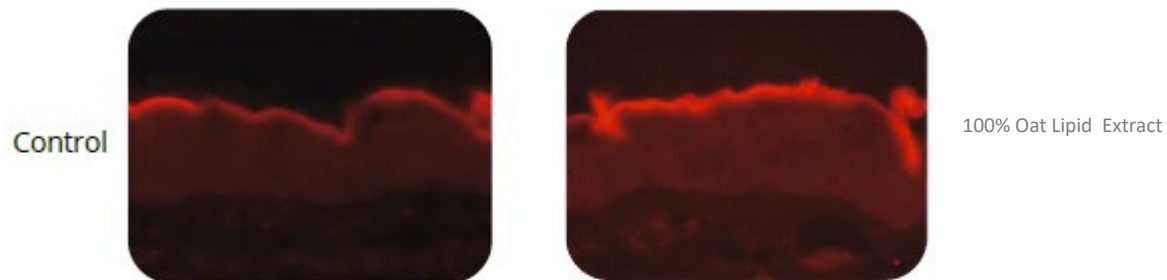


Figure 4: Percentage of surface occupied by neutral lipids in the stratum corneum at Day 5  
(Significant: \* $=p<0.05$  (95%), # $=p<0.1$  (90%))



### Measurement of Polar Lipid Surface at Day 1



### Measurement of Polar Lipid Surface at Day 5

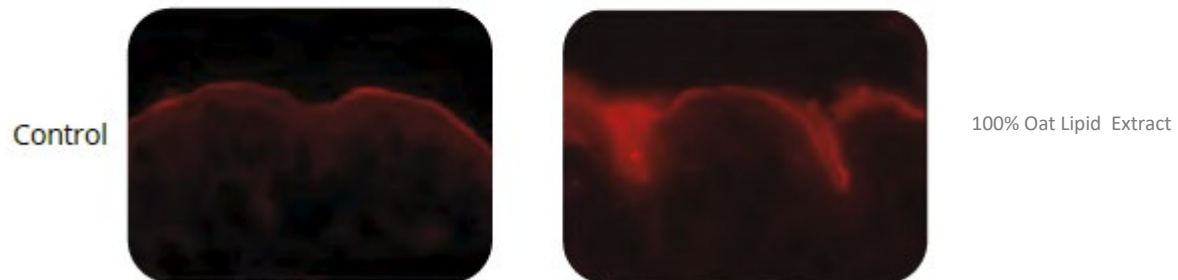
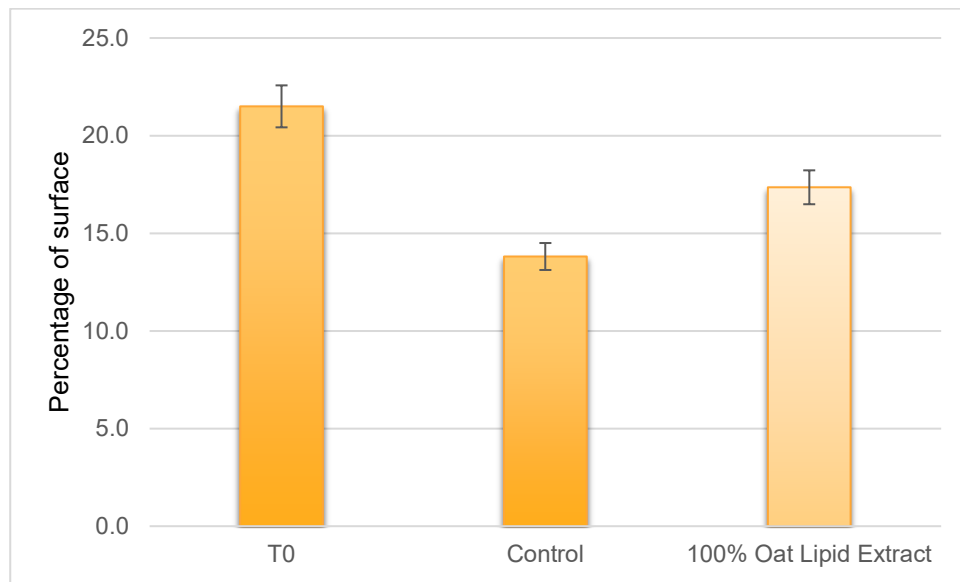


Figure 5: Percentage of surface occupied by polar lipids in the stratum corneum at Day 1 and Day 5 (Significant: \*= $p<0.05$  (95%), #= $p<0.1$  (90%))





### Measurement of the Ceramide Surface at Day 1



Figure 6: Percentage of surface occupied by Ceramides in the stratum corneum at Day 1  
(Significant: \*= $p<0.05$  (95%), #= $p<0.1$  (90%))

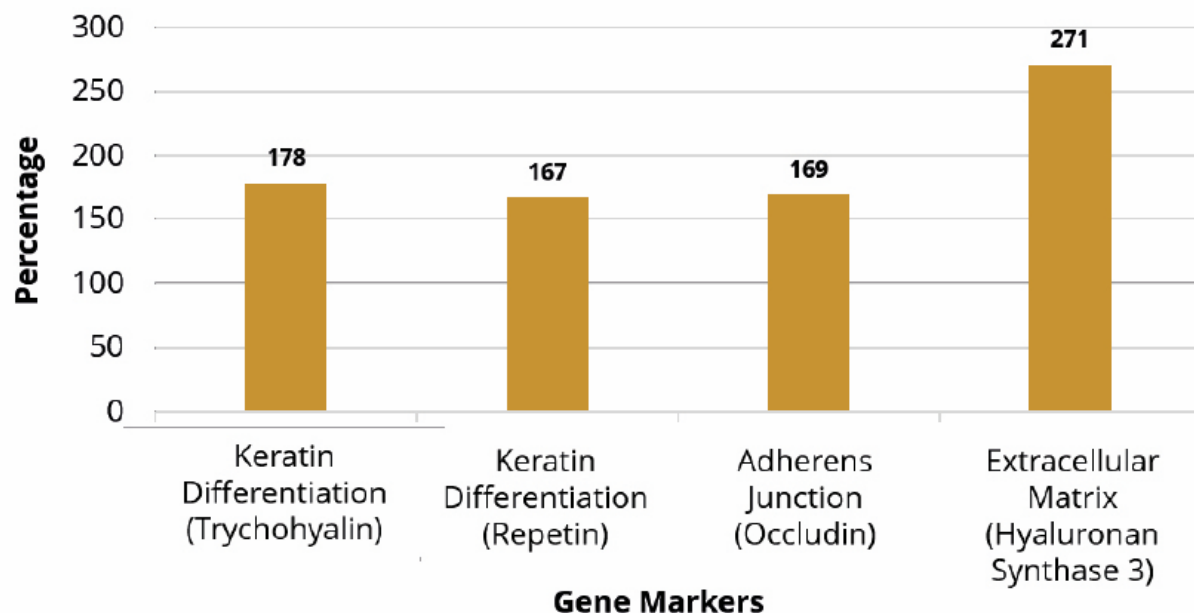
### Barrier Function - Gene Expression

In the MTT assay, there was no negative effect on cell viability (data not shown). The reference retinoic acid, systemically applied at 0.5  $\mu$ M for 72 hours, had a de-differentiating effect on reconstructed human epidermis (RHE) by clearly inhibiting the expression of some late keratinocyte differentiation markers (FLG, LOR), lipid synthesis markers (CERS6, HMGCR), adherens junction markers (CDSN, DSG1, DSC1) and tight junction markers (CLDN1, CGN). In parallel, there was an up-regulation of the expression of markers involved in inflammation (IL8), cornification and desquamation (TCHH, CRCT1, SPRR1B, and SPRR1A), hydration (AQP3) and a regulator of hyaluronan synthesis (HAS3). These results were expected and validated the assay (data not shown).

The Oat Lipid Extract when topically applied, induced a slight up-regulation of the gene expression of HAS3 (Hyaluronan synthase 3 which is involved in the synthesis of the hyaluronic acid, a major constituent of extracellular matrix). In a lesser extent, the effect was also observed after systemic application. When the Oat Lipid Extract was compared to standard oat oil, the lipid extract increased the performance of a number of gene markers (Fig 7). This finding was attributed to the Oat Lipid Extract's unique ratio of polar to non-polar lipids.



## Percentage Increase in Gene Stimulation by Oat Lipid Extract Compared to Oat Oil



Gene Markers	Gene Stimulation Compared to Control	
	Oat Oil (0.017%)	Oat Lipid Complex (0.005%)
Keratin Differentiation (Trychohylan)	87	155
Keratin Differentiation (Repetin)	69	115
Adherens Junction (Occludin)	81	137
Extracellular Matrix (Hyaluronan Synthase 3)	83	225

Figure 7: Effect of Oat Lipid Extract on differentiation and hydration gene markers compared with standard oat oil.

## Electron Microscopy (Lipbarvis®) Analysis

TEM (nICLL)			
	Original Data		<b>p value *</b>
	<b>mean</b>	<b>SD</b>	
<b>untreated</b>	204	21.5	<b>0.0276</b>
<b>Oat Lipid Extract Facial Serum</b>	231	17.4	

Table III: Lipbarvis® TEM: length of lipid lamella per 1000 nm<sup>2</sup> intercellular space (nICLL). Mean and standard deviation (SD) of original data, n=6. \*-significant data

In the treatment of skin and preparation of the suction blisters there were no adverse events recorded and no volunteer drop-outs over the 8-week study period. At 8 weeks of regular product use the mean values of Lipbarvis® transmission electron microscopy (TEM) increase from 204 nm ( $\pm 21.5$  nm) to 231 nm ( $\pm 17.4$ )/1000 nm. An 8-week treatment with Oat Lipid Extract resulted in statistically significantly higher values of intercellular lipid lamellae (nICLL), i.e., an improved skin barrier function in comparison to the untreated test site ( $p = 0.0276$ ). The data relative to untreated an improvement of 14% could be observed to the test site treated with Oat Lipid Extract. The original data of the mean values of the normalized nICLL in the intercellular space (ICS) are given in Table III , and images in Figure 8. The analyzed data were normally distributed, and a t-test for dependent samples were carried out to test the difference between the test sites.

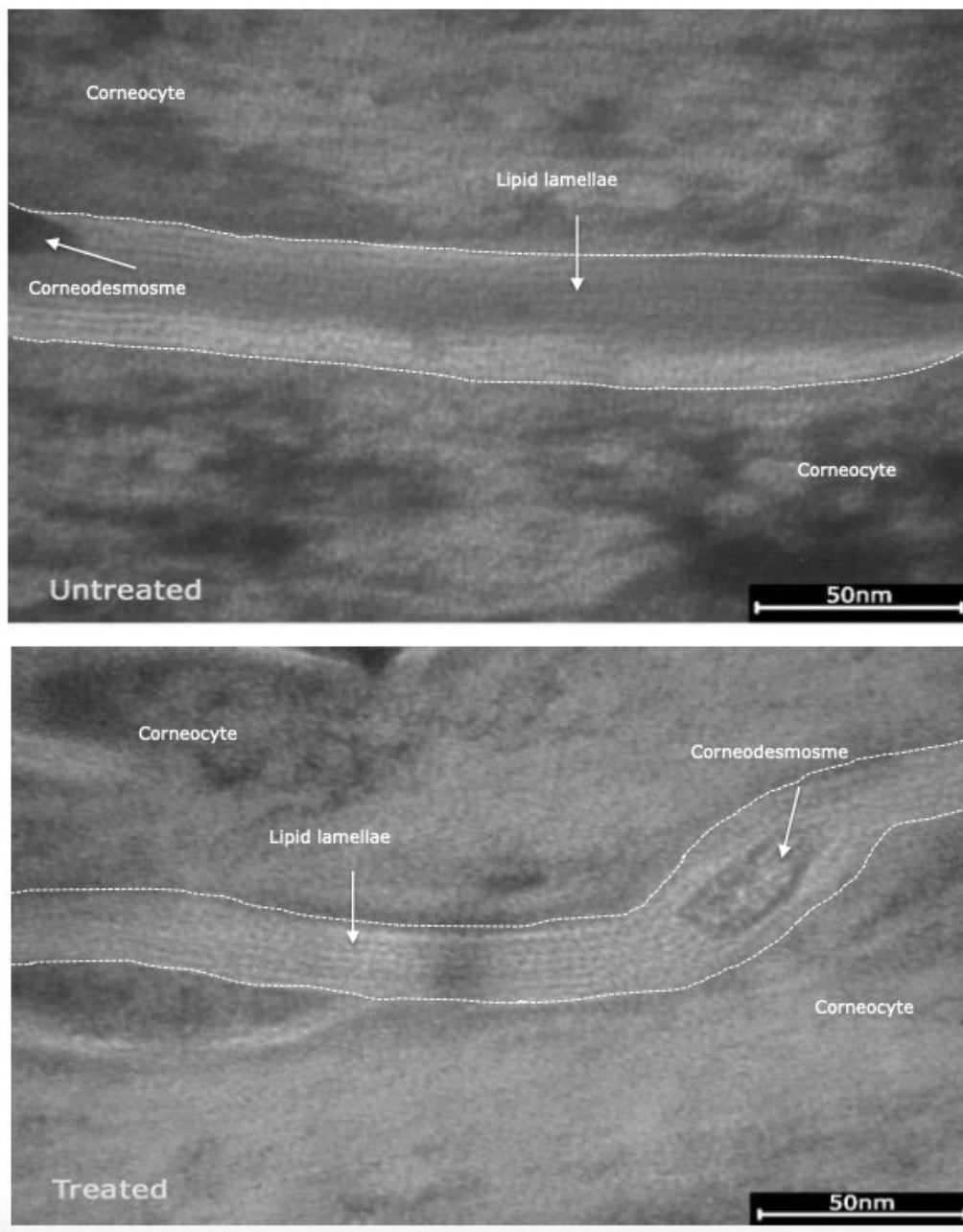


Figure 8:  
TEM  
images of  
the

intercellular space (marked with the dotted lines) between the corneocytes in the stratum corneum of the suction blister samples. The intercellular space is filled with the lipid lamellae (arrow) and is covered by two different corneocytes. In the treated samples the amount of the intercellular lipid lamellae is increased, and the lipid lamellae show more organized and with smaller distances between the lamellae, compared to the untreated samples. This indicates an improved quality of the epidermal barrier.

## Hyaluronic Acid Immunostaining

Hyaluronic Acid			
	Original Data		<b>p value *</b>
	Mean	SD	
<b>Untreated</b>	100852	44471.3	
<b>Oat Lipid Extract Facial Serum</b>	113995	49507.6	<b>0.0040</b>

Table IV: Relative fluorescent of hyaluronic acid values, mean and standard deviation (SD) of original data, n=6 (\*statistically significant)

The mean value of relative fluorescence in hyaluronic acid of the untreated epidermis was 100852 pixels compared to 113995 pixels of the Oat Lipid Extract treated epidermis (Table IV).

The increase in relative fluorescent in hyaluronic acid after product treatment (by 10%) eight weeks was statistically significant ( $p=0.0040$ ). The data relative to the untreated site, an improvement of 14% could be observed to the test site treated with Oat Lipid Extract. Fluorescence imaging of the immuno-labelling of hyaluronic acid of the treated and untreated test-site is given in Figure 9.

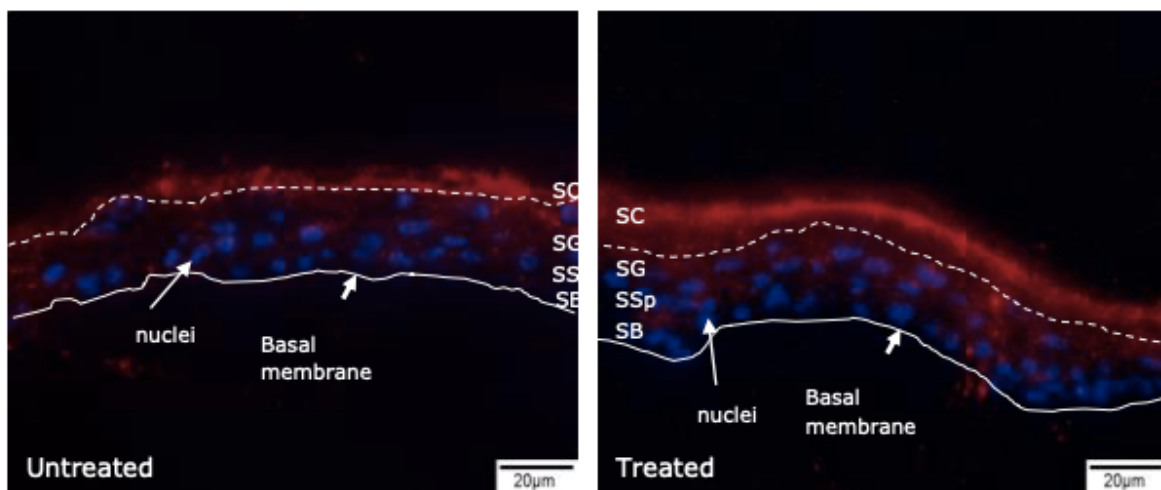


Figure 9: Hyaluronic acid fluorescence staining. Untreated: test site without product treatment, Treated: Oat Lipid Extract treatment twice daily for 8 weeks. Observations show

the immunofluorescence labelling of hyaluronic acid (red) and nuclei staining (blue) in semithin sections of the suction blister samples. In both samples (treated and untreated) the red fluorescence labelling is clearly detectable in all layers (stratum corneum (SC), stratum granulosum (SG) stratum spinosum (SSp) and stratum basale (SB)) of the epidermis. The basal membrane and the interface between SG and SC are marked by lines. The intensity of fluorescence in the treated samples is significant higher than in the untreated samples.

### Occludin Immunostaining

Occludin			
	Original Data		<b>p value</b>
	<b>mean</b>	<b>SD</b>	
<b>Untreated</b>	130778	59913.8	
<b>Oat Lipid Extract Facial Serum</b>	132128	60686.8	0.5685

Table V: Occludin values, mean and standard deviation (SD) of original data, n=6

The mean value of relative fluorescence in occludin of the untreated epidermis was 130778 pixels compared to 132128 pixels of the product-treated epidermis (Table V). An eight-week treatment with Oat Lipid Extract resulted in no statistically significant differences between the treated and untreated test site regarding the parameter occludin ( $p = 0.5685$ ).

Fluorescence imaging of the immuno-labelling of occludin of the treated and untreated test-site is given in Figure 10:

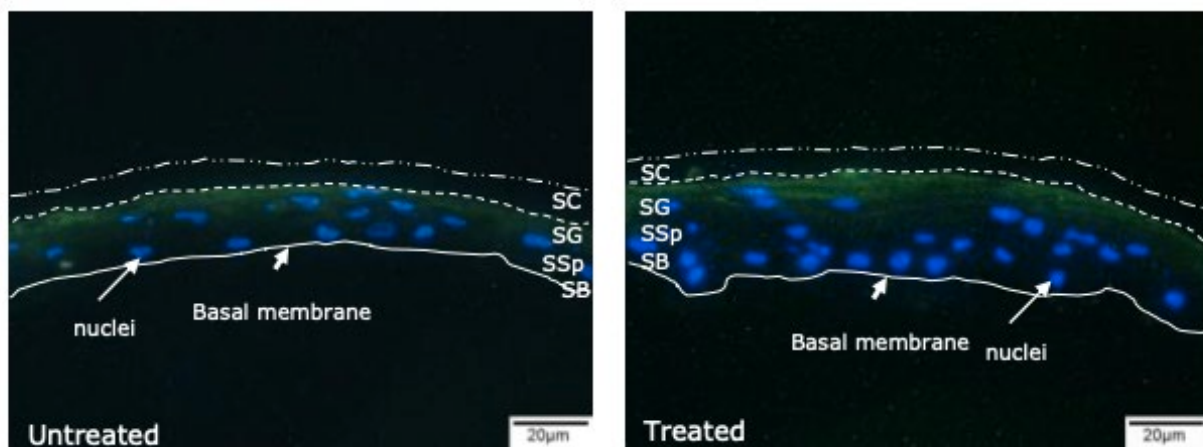


Figure 10: Occludin fluorescence staining. Untreated: test site without product treatment, Treated: Oat Lipid Extract twice daily for 8 weeks. This figure shows the immunofluorescence labelling of occludin (green) and nuclei staining (blue) in semithin sections of the suction blister samples. In both samples (treated and untreated) the green fluorescence is distributed over the middle layers of the epidermis. In all layers of the middle epidermis (SG & SSp) occluding were labelled by the antibody, whereas in the SC no fluorescence signals are detectable, due to the fact that are no tight junctions there. The basal membrane and the interface between SG and SC are marked by lines. The intensity of fluorescence in the treated samples is not significant higher as in the untreated samples.

### Ceramide Immunostaining

Ceramides			<b>p value *</b>	
	Original Data			
	<b>mean</b>	<b>SD</b>		
<b>Untreated</b>	182373	80998.0		
<b>Oat Lipid Extract Facial Serum</b>	202083	90776.8	<b>0.0107</b>	

Table VI: Ceramides values, mean and standard deviation (SD) of original data, n=6 (\*statistically significant)

The mean value of relative fluorescence in ceramides of the untreated epidermis was 182373 pixels compared to 202083 pixels of the product-treated epidermis. An eight-week

treatment with Oat Lipid Extract resulted in statistically significantly higher values of ceramides, i.e., an improvement in comparison to the untreated test site ( $p = 0.0107$ ). The data relative to the untreated site, an improvement of 10% could be observed to the test site treated with Oat Lipid Extract (Table VI).

Fluorescence imaging of the immuno-labelling of ceramides of the treated and untreated test-sites is given in Figure 11.

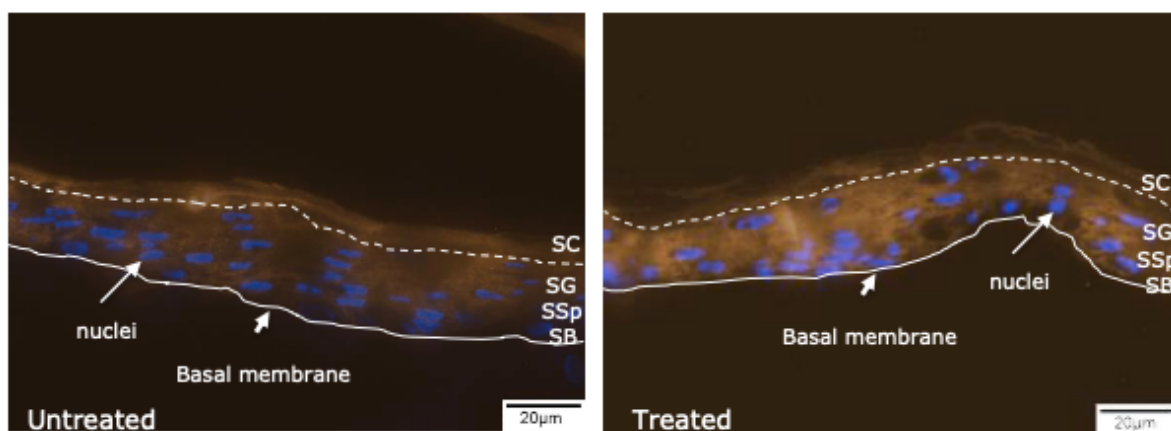


Figure 11: Ceramides fluorescent staining. Untreated: test site without product treatment, Treated: Oat Lipid Extract treatment twice daily for 8 weeks. Observations show immunofluorescence labelling of the ceramides (yellow) and nuclei staining (blue) in semithin sections of the suction blister samples. In both samples (treated and untreated) the yellow fluorescence is distributed over the whole epidermis. In the lower layers of the epidermis (SSp & SG) mostly glycosylceramides are labelled whereas in the SC only ceramides are labelled. The basal membrane and the interface between SG and SC are marked by lines. The intensity of fluorescence in the treated samples is significant higher as in the untreated samples.

## Discussion

This is the first known investigation to date utilising confocal Raman spectroscopy for the identification of oat lipids from *Avena sativa* in viable skin (explants) combined with transmission electron microscopy of the lipid lamellar structures, immunostaining and image analysis of the location and deposition of the various components present in the OAT LIPID EXTRACT. The increasing interest in plant lipids for skin care benefit is a given, and lipid EXTRACTes containing profiles which can mimic or enhance those

present in the skin's barrier are highly sought after. The beneficial effects of oat extracts, especially colloidal oat, on the skin are well documented, notably in the management of dry irritated skin, eczema, and other atopic conditions [34,35]. The role of oat lipids on the skin is however, not so well documented, despite interesting reports of the activity of oat lipid extracts [21,22,]. The objective, therefore, of the investigations described herein was to gain an understanding of the composition and attributes of a specific oat lipid EXTRACT (*AvenaPLex*) by utilising confocal Raman spectroscopy, lipid profiling with GLC-HPTLC, electron microscopy, and the immunostaining of human skin explants.

Our findings have shown that the Oat Lipid Extract extracted from *Avena sativa*, is interesting in its composition, containing phytoceramides, and a significant proportion of those ceramide classes which are also found in human skin (Table 2). The barrier of the skin resides mainly in the SC, and depletion or disturbance in ratio or composition of the free fatty acids, cholesterol and ceramides will result in a disruption of skin barrier function. Several skin disorders are known to have a disturbed barrier functioning [36] such as atopic dermatitis, which has been reported to improve by treatment with a combination of colloidal oat and oat oil [34]. During the course of ageing, ceramides, especially the phytosphingosine ceramides, also become deficient, therefore, it is of importance to understand the interrelationship between the depletion of SC lipids and skin diseases as well as factors that affect the composition and organization of SC lipids in order to assess the potential benefit of a direct replacement of the missing SC lipids as a means of treating disturbed skin barrier conditions [37, 38].

Our findings show the presence of both non-hydroxy-phytosphingosine (NP) and alpha-hydroxy-phytosphingosine (AP) and are indicative of potential barrier improvement, which we demonstrated via immunostaining and Raman analysis. Furthermore, the presence of these and other skin identical ceramides (Table 2) support data reported in *Avena abyssinica* [21,22]. Raman profiling requires further analysis in order to get a more accurate estimation of the effect on the ratios of the fluid state and liquid crystalline states of the orthorhombic packing. The clear increase in stratum corneum total ceramide content by the oat lipid EXTRACT was significant ( $p < 0.05$ ) suggesting a positive benefit on skin barrier functioning. This was verified in a separate proof-of-principle study whereby transepidermal water loss (TEWL) was significantly reduced over a two-hour period in dry skinned individuals versus a vehicle formulation (authors unpublished data). While further work is in progress, we suggest that replenishment or replacement of missing lipids, or

even enhancing their synthesis in the SC, could be used to treat disturbed skin barrier conditions.

Regarding the Lipbarvis® TEM and immunostaining, in vivo application of Oat Lipid Extract twice daily for eight weeks resulted in a statistically significant increase in the length of the intercellular lipid lamellae in the stratum corneum and the amount of detectable hyaluronic acid and ceramides in the epidermis (Stratum corneum, Stratum granulosum, Stratum spinosum). The increasing in the length of the intercellular lipid lamellae in the stratum corneum correlates with stronger fluorescence signal in the immunolabelling of the ceramides in the epidermis. The so called “second barrier” which are represented by the tight junctions in the epidermis and the marker protein occluding investigated for this purpose seem unaffected by the product application. We surmise that the increased content of hyaluronic acid should also be contributing to improved hydration in the epidermis.

Interestingly, the preliminary gene array study demonstrates the ability of Oat Lipid Extract to up-regulate hyaluronan synthase. Since hyaluronan metabolism in human keratinocytes and atopic dermatitis is driven by a balance between hyaluronan synthases 1 and 3 [39], our finding warrants further investigation in terms of the implications for atopic benefits by Oat Lipid Extract.

Further investigative work is planned to understand and quantify the ability of oat lipid EXTRACT to supplement and restore skin barrier lipids. How Oat Lipid Extract exhibits atopic benefits is also of interest in light of the up-regulation of hyaluronan synthase. Currently, we have completed a theoretical feasibility study to determine which oat complex lipids are detectable in the skin and further work is being progressed to evaluate the effect of these oat lipids have on skin lipids in vivo. Limitations lie in the fact that endogenous ceramides and exogenous ceramides are to date indistinguishable from each other, and even tagging exogenous ceramides risks metabolic breakdown.

## Conclusions

Oat ceramides in the form of Oat Lipid Extract can be effectively delivered into the stratum corneum and are proven to be a good source of skin supplementing lipids. Our profiling has shown that Oat Lipid Extract is unique in its composition, containing phytoceramides, and a significant proportion of the ceramide classes required by the skin. This unique ratio is indicative of skin barrier improvement, which we have demonstrated via

immunostaining, Raman analysis, Lipbarvis® TEM and immunostaining, as well as showing an up-regulation hyaluronan synthase through a gene array study.

Further studies are required to provide evidence of the liquid crystalline changes that occur, and the molecular arrangement in the stratum corneum remains to be investigated. This preliminary Raman study has given good insight into the possibility of Oat Lipid Extract mimicking the structure and function of the skin's barrier.

## Acknowledgements

The authors would like to thank Dr Theresa Callaghan, Callaghan Consulting International, Hamburg, Germany for the preparation of this manuscript and helpful discussions.

## References

1. Madison C. Barrier function of the skin: "La raison d'etre "of the epidermis. *J. Invest Dermatol.* **121**, 231 - 241 (2003)
2. Bouwstra J, Ponec M. The skin barrier in healthy and diseased state. *Biochim Biophys Acta.* **1758**, 2080-2095 (2006).
3. Kahraman E, Kaykın M, Bektay H, Güngör S. Recent advances on topical application of ceramides to restore barrier function of skin. *Cosmetics* **6**: 52 (2019).  
doi:10.3390/cosmetics6030052
4. Das C, Olmsted P. The physics of stratum corneum lipid membranes *Phil. Trans. R. Soc. A* **374**: 20150126 (2016)
5. Badhe Y, Gupta R, Rai B. Structural and barrier properties of the skin ceramide lipid bilayer: a molecular dynamics simulation study. *J. Mol Model.* **25**, 140 (2019)
6. Wang E, Klauda J. Models for the stratum corneum lipid matrix: effects of ceramide concentration, ceramide hydroxylation, and free fatty acid protonation. *J. Phys. Chem B.* **122**, 11996-12008 (2018).

7. Mojumdar E, Gooris G, Bouwstra J. Phase behavior of skin lipid mixtures: the effect of cholesterol on lipid organization. *Soft Matter*. **11**, 4326-36 (2015).
8. Janssens M, van Smeden J, Gooris G, Bras W, Portale G. et al. Increase in short-chain ceramides correlates with an altered lipid organization and decreased barrier function in atopic eczema patients. *J. Lipid Res.* **53**, 2755 - 2766 (2012).
9. Bouwstra J, Dubbelaar F, Gooris G, Weerheim A, Ponec M. The role of ceramide composition in the lipid organisation of the skin barrier *Biochim. Biophys. Acta* **1419**, 127-136 (1999)
10. Garibyan L, Chiou, A, Elmariah S. Advanced aging skin and itch: addressing an unmet need. *Dermatol Ther* **26**: 92–103 (2013).
11. van Smeden J, Bouwstra J. Stratum corneum lipids: their role for the skin barrier function in healthy subjects and atopic dermatitis patients. *Curr Probl Dermatol*. **49**, 8-26 (2016)
12. Behne M, Uchida Y, Seki T, Ortiz de Montellano P, Elias P, Holleran W. Omega-hydroxyceramides are required for corneocyte lipid envelope (CLE) formation and normal epidermal permeability barrier function. *J. Invest Dermatol* **114**:185-192 (2000).
13. Zheng Y, Yin H, Boeglin W, Elias P, Crumrine D. et al. Lipoxygenases mediate the effect of essential fatty acid in skin barrier formation. *J. Biol. Chem.* **286**: 24045-24056 (2011).
14. Tessemaa E, Gebre-Mariam T, Neubert R, Wohlrabb J. Potential applications of phyto-derived ceramides in improving epidermal barrier function. *Skin Pharmacol. Physiol.* **30**, 115–138 (2017)
15. Lin T-K, Zhong L, Santiago J-L. Anti-inflammatory and skin barrier repair effects of topical application of some plant oils . *Int. J. Mol. Sci.* **19**, 70 (2018)
16. Vaughn A, Clark A, Sivamani R,3, Shi V. Natural oils for skin barrier repair: ancient compounds now backed by modern science. *Am J Clin Dermatol.* **19**, 103-117 (2018)
17. Shimoda H, Terazawa S, Hitoe S, Tanaka J, Nakamura S, et al. Changes in ceramides and glucosylceramides in mouse skin and human epidermal equivalents by rice-derived glucosylceramide. *Med Food.* **15**,1064-72 (2012)

18. Bizot V, Cestone E, Michelotti A , Nobile V. Improving skin hydration and age-related symptoms by oral administration of wheat glucosylceramides and digalactosyl diglycerides: a human clinical study. *Cosmetics* **4**, 37-53 (2017)
19. Soycana G, Schära M, Kristeka A, Boberskaa J, Alsharif S. et al. Composition and content of phenolic acids and avenanthramides in commercial oat products: Are oats an important polyphenol source for consumers? *Food Chemistry X* **3**, 100047 (2019)
20. Singh R, De S, Belkheir A. *Avena sativa* (Oat), a potential nutraceutical and therapeutic agent: an overview. *Crit Rev Food Sci Nutr.* **53**, 126-44. (2013)
21. Tessema E, Gebre-Mariam T, Lange S, Dobner B, Neubert R. Potential application of oat-derived ceramides in improving skin barrier function: Part 1. Isolation and structural characterization. *J Chromatogr B Analyt Technol Biomed Life Sci.* **1065-1066**, 87-95 (2017)
22. Chon S, Tannahill R, Yao X, Southall M, Pappas A. Keratinocyte differentiation and up-regulation of ceramide synthesis induced by an oat lipid extract via the activation of PPAR pathways. *Exp. Dermatol.* **24**, 290-295 (2015)
23. Falcone D, Uzunbajakava N, Varghese B, de Aquino Santos G, Richters R, et al. Microspectroscopic confocal Raman and macroscopic biophysical measurements in the in vivo assessment of the skin barrier: perspective for dermatology and cosmetic sciences. *Skin Pharmacol Physiol.* **28**, 307-317 (2015)
24. Böhling A, Bielfeldt S, Himmelmann A, Keskin M, Wilhelm KP. Comparison of the stratum corneum thickness measured in vivo with confocal Raman spectroscopy and confocal reflectance microscopy. *Skin Res Technol.* **20**, 50- 57 (2014).
25. Förster M, Bolzinger M, Montagnac G, Briançon S. Confocal Raman microspectroscopy of the skin. *Eur J Dermatol.* **21**, 851-863 (2011)
26. Tfayli A, Bonnier F, Farhane Z, Libong D, Byrne HJ, Baillet-Guffroy A. Comparison of structure and organization of cutaneous lipids in a reconstructed skin model and human skin: spectroscopic imaging and chromatographic profiling. *Exp Dermatol.* **23**, 441-443 (2014)
27. Christie, W. *Lipid Analysis*, 3rd Edition; The Oily Press, Bridgewater, UK. 205-224 (2003)

28. Ackman, R. Fish lipids. In: Connell, J. (Ed.), *Advances in Fish Science and Technology*: Fishing News Books: Farnham 83-103. (1980)
29. Yang Z, Piironen V, Lampi A. Epoxy and hydroxy fatty acids as non-volatile lipid oxidation products in oat. *Food Chem.* **295**, 82-93 (2019)
30. Vyumuuhore R, Tfayli A, Duplan H, Delalleau A, Manfait M, Baillet-Guffroy A. Effects of atmospheric relative humidity on stratum corneum structure at the molecular level: ex vivo Raman spectroscopy analysis. *Analyst* **138**, 4103-4111 (2013)
31. Peno-Mazzarino L. The Missing Bridge between ex vivo and in vivo Models: The Perfex Vivo System. Proceedings of the IFSCC Congress (18-21 September), Munich Germany (2018)
32. Goldner J. A modification of the Masson trichome techniques for routine laboratory purposes. *Amer. J. Pathol* **14**, 237-243 (1938)
33. Sadowski T, Klose C, Gerl M, Wójcik-Maciejewicz A, Herzog R. et al. Large-scale human skin lipidomics by quantitative, high-throughput shotgun mass spectrometry. *Scientific Reports* **7**, 43761, (2017)
34. Reynertson K, Garay M, Nebus J, Chon S, Kaur S. et al. Anti-inflammatory activities of colloidal oatmeal (*Avena sativa*) contribute to the effectiveness of oats in treatment of itch associated with dry, irritated skin. *J Drugs Dermatol.* **14**, 43-48 (2015)
35. Fowler J. Colloidal oatmeal formulations and the treatment of atopic dermatitis. *J Drugs Dermatol.* **13**, 1180-1183 (2014)
36. Sahle F, Gebre-Mariam T, Dobner B, Wohlrab J, Neubert R. Skin diseases associated with the depletion of stratum corneum lipids and stratum corneum lipid substitution therapy. *Skin Pharmacol Physiol.* **28**:42–55 (2015).
37. Wang Z, Man M-Q, Li T, Elias P, Mauro T. Aging-associated alterations in epidermal function and their clinical significance. *Aging* **12**: 5551-5565 (2020).
38. Trayssac M, Hannun Y, Obeid L. Role of sphingolipids in senescence: implication in aging and age-related diseases. *J. Clin. Invest.* **128**:2702–2712 (2018).

39. Malaisse J, Bourguignon V, De Vuyst E, Lambert de Rouvroit C, Nikkels A. et al.  
Hyaluronan metabolism in human keratinocytes and atopic dermatitis skin is driven by a  
balance of hyaluronan synthases 1 and 3. *J. Invest. Dermatol.* **134**, 2174-2182 (2014)